

Ultrafast charging of LiFePO₄ with gaseous oxidants under ambient conditions†

Cite this: *Chem. Sci.*, 2013, **4**, 4223

Christian Kuss,^a David Lepage,^a Guoxian Liang^b and Steen B. Schougaard^{*a}

Lithium iron phosphate is a lithium-ion battery positive electrode material with widespread use, as well as, unusually complex redox chemistry. Here we report on the discovery of a direct gas–solid delithiation reaction. Unique to this reaction, in addition to the lack of solvent, is remarkably fast kinetics. *In situ* X-ray diffraction, corroborated by elemental analysis, shows for the first time that LiFePO₄ bulk diffusion supports nearly complete delithiation/charging of carbon coated LiFePO₄ micropowder at ambient temperature in less than 60 seconds.

Received 2nd May 2013
Accepted 19th August 2013

DOI: 10.1039/c3sc51195b

www.rsc.org/chemicalscience

Introduction

Electric cars are back on the mass market as an environmentally friendly mode of personal transportation. However, current consumers are cautious and have voiced concerns about long charging times which limits autonomy.¹ Importantly, speed of charge is related to slow transport kinetics inside the battery. This is, in turn, often associated with the kinetics of the lithium insertion/deinsertion reaction in the ceramic electroactive solid, since solid-state diffusion generally is slow compared to the liquid and the gas phase.² Specifically, LiFePO₄ though superior in many aspects to other positive electrode materials, is criticized for low electronic conductivity and bulk lithium diffusivity.³ Yet, in model systems, LiFePO₄ electrode materials repeatedly exhibit a much larger diffusion coefficient (around 10⁻⁸ cm² s⁻¹)^{4,5} than in LiFePO₄ powders designed for application (around 10⁻¹⁴ cm² s⁻¹).² Moreover, a limited number of experimental results have recently shown that commercially relevant LiFePO₄ might be capable of much higher charge/discharge rates, than previously thought. For example, Ceder and co-workers published a controversial⁶ study on a modified LiFePO₄ material with non-stoichiometric composition and amorphous surface layer, with which approximately 75% of the theoretical capacity could be achieved within a one minute discharge.⁷ Similarly an electrochemical single particle study by Munakata and co-workers showed about 75% of the initial capacity at a one minute discharge.⁸

At the same time, industry is concerned with the stability of LiFePO₄ in ambient atmosphere, as this is of great importance to the storage and handling of commercial LiFePO₄ during production. For example, complete transformation of LiFePO₄ into the NASICON analogue Li₃Fe₂(PO₄)₃ and hematite was observed during exposure to air at 300 °C and above,⁹ whereas at temperatures below 120 °C, in humid air, the formation of hydroxide containing compounds has been reported.^{10,11} Yet, it remains unclear, why lithium is *not* extracted under oxidative aging conditions, even though this is the dominating mode of oxidation in solution.

To address this question of different reaction modes in air compared to electrolyte, and to shed light on the lithium transport kinetics of these reactions, we have examined the impact of different gaseous oxidants on commercial LiFePO₄. Surprisingly, we have found that even though exposure to O₂/O₃ did *not* significantly alter the LiFePO₄ materials, NO₂ consistently delithiates LiFePO₄ completely within a short period of time according to the following reaction:



This reaction differs significantly from previous oxidative delithiation transformations, as it does not include a liquid phase that can solvate the lithium ion and transport it away from the surface as the reaction progresses. More importantly, it exhibits unseen fast reaction rates for commercial LiFePO₄ materials.

Results and discussion

Characterization

To confirm, that this reaction indeed is comparable to electrochemical charging, the solid reaction products have been characterized using attenuated total reflectance infrared

^aDépartement de Chimie, Université du Québec à Montréal, Case postale 8888 Succ. Centre-ville, Montréal, (QC) H3C 3P8, Canada. E-mail: schougaard.steen@uqam.ca; Fax: +1 514-987-4054

^bClariant Canada, Inc., 1475, rue Marie-Victorin, St-Bruno de Montarville, (QC) J3V 6B7, Canada

† Electronic supplementary information (ESI) available: Experimental information and discussion of gas oxidation thermodynamics. See DOI: 10.1039/c3sc51195b

spectroscopy (ATR-FTIR), X-ray diffraction (XRD), electrochemical cycling and transmission electron microscopy.

After treatment of carbon-coated LiFePO_4 (C-LiFePO₄) micropowders with NO_2 , evidence of delithiation was given by LiNO_3 and *heterosite* FePO_4 as identified by ATR-FTIR and XRD (Fig. 1c and f). Specifically, the LiNO_3 gives rise to FTIR bands at 737, 838, 1072, 1135 cm^{-1} and a broad feature between 1300 and 1500 cm^{-1} , as well as a number of shoulders, which appear in addition to the standard *heterosite* FePO_4 spectrum (Fig. 1f).¹⁵

The completeness of the delithiation was confirmed by atomic emission spectroscopy (AES): $100 \pm 3\%$ lithium was extracted, while $2 \pm 1\%$ lithium remained in the washed FePO_4 sample.

As the use of aggressive oxidants to delithiate LiFePO_4 might lead to the formation of non-crystalline by-products or particle dissolution, high-resolution transmission electron micrographs of nano-sized carbon-free LiFePO_4 were recorded to assess structural integrity of the reaction product. From Fig. 2, it is clear that the overall shape, size and appearance of the particles remain unaltered. Furthermore, FePO_4 particles remain crystalline while a salt layer forms non-uniformly on the surface, accumulating in gaps and contact points. X-Ray photoelectron spectroscopy reveals a nitrogen containing compound on the material surface. Fig. 3 shows the N 1s peak at 406.7 eV, lying in

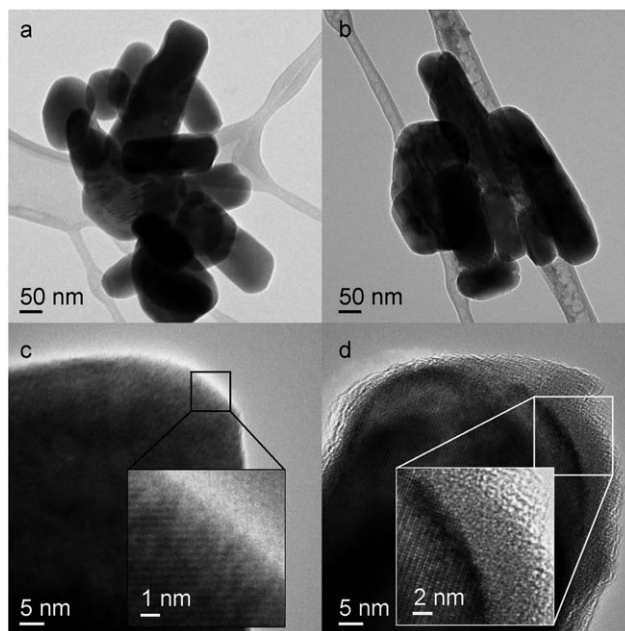


Fig. 2 TEM images of LiFePO_4 before oxidation (a and c) and after oxidation with nitrogen dioxide (b and d). HRTEM images show crystallinity of particles up to the surface before oxidation (c) and an amorphous surface layer after oxidation (d).

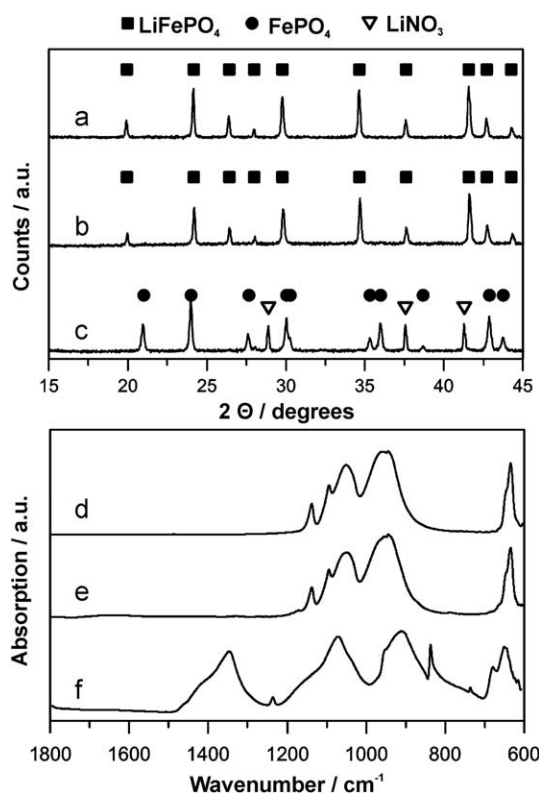


Fig. 1 Crystallographic and chemical analysis of the reaction product of C-LiFePO₄ with O_3 and NO_2 . X-ray diffractograms (a–c) and ATR FTIR spectra (d–f) of pristine C-LiFePO₄ (a and d), O_3 exposed C-LiFePO₄ (b and e) and NO_2 oxidized C-LiFePO₄ (c and f). The symbols mark the location of strong reflections according to literature crystallographic data.^{12–14}

between the values reported for AgNO_3 ¹⁶ and NH_4NO_3 ,¹⁷ thus suggesting the presence of LiNO_3 on the surface. The same references report O 1s peaks at 532.3 and 532.5 eV, which compares well to the observed component at 532.4 eV.

The electrochemical activity of oxidized C-LiFePO₄ was assessed in research coin cell batteries, assembled with great care to avoid any accidental short-circuit. Electrochemical testing was initiated in discharge mode, without prior charging. This first discharge (Fig. 4a) indicates a stable potential plateau

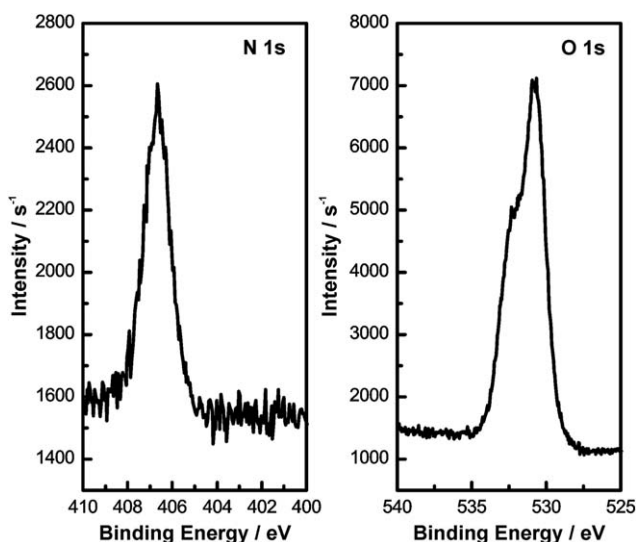


Fig. 3 XPS analysis of the nitrogen and oxygen 1s peaks of the oxidized sample confirms the presence of LiNO_3 at the surface.

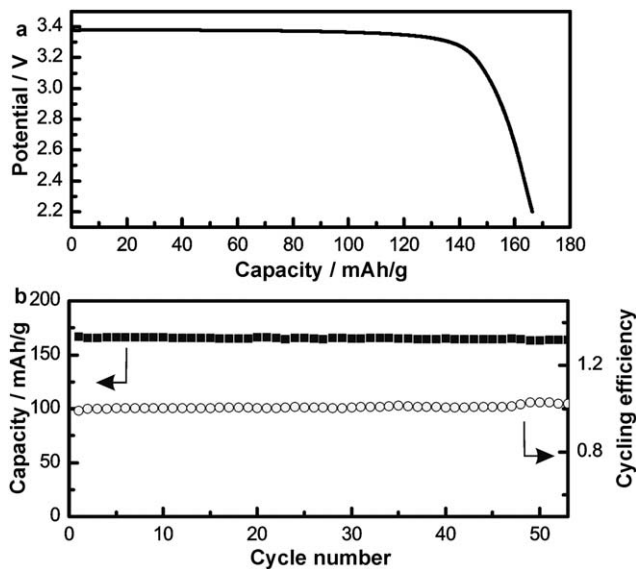


Fig. 4 (a) First-cycle discharge curve (rate C/10) and (b) cycling performance (rate C/2) of oxidized, washed and dried C-LiFePO₄ confirm complete oxidation and retention of electrochemical activity of the oxidized material.

around 3.4 V vs. Li/Li⁺ and practical capacity of 165 mA h g⁻¹ (theoretical capacity: 170 mA h g⁻¹). Combined with the cycling stability over 50 cycles (Fig. 4b), this indicates that the material retains its electrochemical properties and is not damaged by the aggressive delithiation.

As mentioned above, LiFePO₄ was also exposed to ozone. This gas did not lead to a significant alteration of the starting material, *i.e.* the bulk *olivine* structure remains intact, as observed in XRD, and further confirmed by only very minor changes to the ATR-FTIR spectrum (Fig. 1b and e).

Thermodynamics of LiFePO₄ delithiations with gases

It is clear, that the key to the observed differentiated reaction behaviours lies within the nature of the oxidant. Table 1 summarizes some reaction Gibbs free energies for delithiation reactions of LiFePO₄ with different oxidizing gases using actual reaction conditions for NO₂, Cl₂ and O₃ oxidations, and ambient conditions for O₂. The thermodynamic discussion of oxidation pathways of LiFePO₄ with gases may further be extended to the

Table 1 Gibbs free energies of delithiation reactions under reaction/ambient conditions^{a,18,19}

Reaction	$\Delta_R G / \text{kJ mol}^{-1}$
$\text{LiFePO}_4 + \frac{1}{2}\text{Cl}_2 \rightarrow \text{LiCl} + \text{FePO}_4$	-53
$\text{LiFePO}_4 + 2\text{NO}_2 \rightarrow \text{LiNO}_3 + \text{FePO}_4 + \text{NO}$	-65
$\text{LiFePO}_4 + \frac{1}{2}\text{O}_3 \rightarrow \frac{1}{2}\text{Li}_2\text{O} + \text{FePO}_4 + \frac{1}{2}\text{O}_2$	-19
$\text{LiFePO}_4 + \frac{1}{2}\text{O}_3 + \frac{1}{2}\text{H}_2\text{O} \rightarrow \text{LiOH} + \text{FePO}_4 + \frac{1}{2}\text{O}_2$	-60
$\text{LiFePO}_4 + \frac{1}{4}\text{O}_2 \rightarrow \frac{1}{2}\text{Li}_2\text{O} + \text{FePO}_4$	+51
$\text{LiFePO}_4 + \frac{1}{4}\text{O}_2 + \frac{1}{2}\text{H}_2\text{O} \rightarrow \text{LiOH} + \text{FePO}_4$	+11
$\text{LiFePO}_4 + \frac{1}{4}\text{O}_2 + \frac{1}{2}\text{CO}_2 \rightarrow \frac{1}{2}\text{Li}_2\text{CO}_3 + \text{FePO}_4$	-38

^a 20 °C, 20.9% O₂, 0.035% of CO₂, and 70% rel. humidity were assumed ambient conditions.

extraction of iron ions from, or introduction of oxygen into the LiFePO₄ structure. However, molecular modelling shows, that those ions are strongly bound to their lattice site in the LiFePO₄ structure, compared to a more mobile lithium.¹⁸ Bulk diffusion kinetics should hence favour delithiation reactions. Delithiation of LiFePO₄ with O₃ and O₂ in the presence of CO₂ is thermodynamically possible with free energies down to -60 kJ mol⁻¹ at standard conditions depending on the pathway.¹⁹ This delithiation is *not* observed, suggesting surface kinetics are responsible for its inhibition *e.g.* surface localized species may block the reaction. Given that ozone is a strongly oxidizing allotrope of oxygen, the reaction products of O₂/LiFePO₄ and O₃/LiFePO₄ may be quite similar, thus potentially yielding new information on the dry air aging mechanism of LiFePO₄.

Kinetics

In an attempt to quantify the exceptionally high reaction rate, *in situ* time-resolved XRD was performed. Fig. 5 shows evidence of

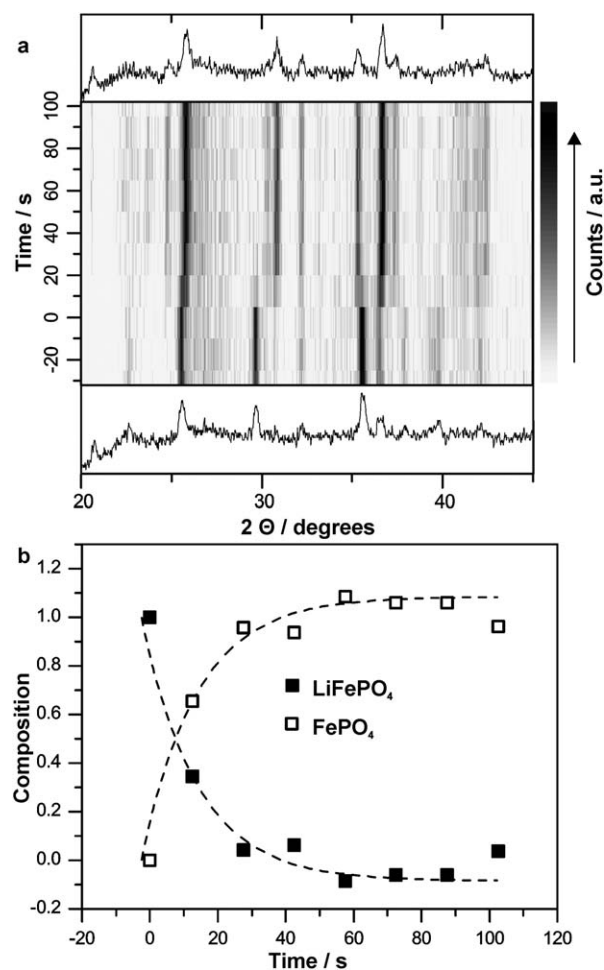


Fig. 5 (a) Time-resolved XRD during delithiation of C-LiFePO₄ by NO₂ gas as a greyscale map. The initial and final diffractograms are displayed at the top and bottom, respectively; $t = 0$ marks the time of gas injection. (b) Composition of the mixture LiFePO₄/FePO₄. The composition was determined from time-resolved XRD by integration and normalization to the corresponding theoretical intensity of the LiFePO₄ reflection at 30° 2θ and the FePO₄ reflection at 31° 2θ (based on a Cu-Kα anode X-ray source).

complete delithiation of C-LiFePO₄ particles of 590 nm average diameter within significantly less time than one minute. The rate of delithiation was also confirmed by AES with 61 ± 14% delithiation at 30 s and 94 ± 4% delithiation at 60 s. This translates into a LiFePO₄ charge to 160 mA h g⁻¹ within one minute. Importantly, the reaction temperature peaked at 29.7 °C ± 1.1 °C, thus excluding any major thermal increase of the kinetics resulting from the exothermic nature of the reaction. Moreover, preliminary tests using C-LiFePO₄ and Cl₂ have shown similar kinetics. LiFePO₄ nanopowder samples of approximately 200 nm average particle diameter with and without carbon coating have been studied as well. Regardless of the presence or absence of coating, these showed reaction rates that were too fast to be captured within the 15 seconds time resolution of this conventional X-ray diffraction set-up.

For comparative purposes, our data provides a *lower limit* on the apparent diffusion coefficient of about 3.1 × 10⁻¹¹ cm² s⁻¹, using a one-dimensional pure diffusion model, as has been done in previous electrochemical studies.²⁰ As such, this study shows that the rates provided by Ceder *et al.*⁷ and Munakata *et al.*⁸ are entirely feasible *provided* that the removal of electrons from the particle surface is sufficiently fast.

Conclusion

Unique to the gas reaction discovered here, is the delithiation of LiFePO₄ at high speed *without* the presence of a liquid. *In situ* X-ray diffraction corroborated by elemental analysis provides proof that LiFePO₄ bulk kinetics supports a charge to 160 mA h g⁻¹ in less than 60 seconds under ambient conditions. This finding has been confirmed with two LiFePO₄ materials resulting from different synthesis routes regardless of the presence or absence of carbon coating. The reaction is comparable to the electrochemical process in so far as the resulting FePO₄ is indistinguishable from electrochemically delithiated Li₀FePO₄ and the thermodynamic driving force corresponds to a charge to 4.1 V vs. Li/Li⁺. It provides thus new possibilities to study the delithiation mechanism of LiFePO₄ *in situ* and *ex situ*. As such, XRD and TEM studies are currently underway. The findings further disprove the paradigm of slow lithium bulk diffusion in LiFePO₄.

In conclusion, the presented data suggest that developing LiFePO₄ materials with improved bulk lithium diffusivity will not improve rate capabilities of the derived lithium-ion batteries. Instead, electrode design, electronic conductivity and surface kinetics should be the focus of continued research.

Experimental

Micro-sized carbon coated LiFePO₄ (C-LiFePO₄, US Pat., 7,457,018) and carbon-free nano-LiFePO₄ (US Pat., 7,807,121 B2) were donated by Clariant (Canada) Inc. (former Phostech Lithium Inc).

C-LiFePO₄ (chemical and crystallographic analysis) and carbon-free nano-LiFePO₄ (used for XPS) samples were exposed to nitrogen dioxide and ozone gas, respectively, for at least 30 minutes. For chemical quantification of the oxidation,

oxidized samples were washed in water and filtered. FePO₄ was subsequently dissolved in conc. HNO₃. Wash water and dissolved FePO₄ were analysed by AES. To achieve time resolution, the oxidation was stopped after different exposure times by replacing NO₂ gas with a stream of dry air. TEM samples were prepared by depositing carbon-free nano-LiFePO₄ onto lacey carbon nickel grids from a suspension in acetonitrile. Selected sample covered grids were exposed to NO₂ gas before analysis in the TEM. Carbon-coated nano-LiFePO₄ shows the same characteristics.

The electrodes for battery testing were produced by coating 85 wt% washed, completely oxidized LiFePO₄, 6 wt% PVDF binder and 9 wt% carbon additive on to a carbon-coated aluminium foil. The battery contained a metallic lithium negative electrode and LiPF₆ in 1 : 1 ethylene carbonate and dimethyl carbonate mixture electrolyte.

Time-resolved X-ray diffraction was performed using a flow of NO₂ gas below a filter paper on which LiFePO₄ was fixed. X-ray access to the XRD cell was enabled through a Kapton window. In similar experiments, the peak temperature of LiFePO₄ during NO₂ oxidation was recorded, using an infrared thermometer and confirmed in independent experiments with a thermocouple.

For more experimental details, suppliers and instruments, please see the ESI.†

Funding

Funding and some material for this research work has been provided by Clariant Canada, Inc., a producer of commercial LiFePO₄ material.

Acknowledgements

The authors acknowledge gratefully technical assistance by Yanis Boukkit (elemental analysis), Michel Preda (XRD), Thierry Maris (time resolved XRD), Jean-Phillipe Masse (TEM), and Pascale Chevallier (XPS) as well as the National Science and Engineering Research Council of Canada (NSERC), Grant no. CRD 385812-09 for financial support. The carbon coated Al foil was kindly donated by Exopack.

Notes and references

- 1 E. Graham-Rowe, B. Gardner, C. Abraham, S. Skippon, H. Dittmar, R. Hutchins and J. Stannard, *Transp. Res., Part A*, 2012, **46**, 140–153.
- 2 M. Park, X. Zhang, M. Chung, G. B. Less and A. M. Sastry, *J. Power Sources*, 2010, **195**, 7904–7929.
- 3 Y. Zhang, Q.-y. Huo, P.-p. Du, L.-z. Wang, A.-q. Zhang, Y.-h. Song, Y. Lv and G.-y. Li, *Synth. Met.*, 2012, **162**, 1315–1326.
- 4 D. Morgan, A. Van der Ven and G. Ceder, *Electrochem. Solid-State Lett.*, 2004, **7**, A30–A32.
- 5 C. Kuss, G. Liang and S. B. Schougaard, *J. Mater. Chem.*, 2012, **22**, 24889–24893.

- 6 K. Zaghib, J. B. Goodenough, A. Mauger and C. Julien, *J. Power Sources*, 2009, **194**, 1021–1023.
- 7 B. Kang and G. Ceder, *Nature*, 2009, **458**, 190–193.
- 8 H. Munakata, B. Takemura, T. Saito and K. Kanamura, *J. Power Sources*, 2012, **217**, 444–448.
- 9 S. Hamelet, P. Gibot, M. Casas-Cabanas, D. Bonnin, C. P. Grey, J. Cabana, J.-B. Leriche, J. Rodriguez-Carvajal, M. Courty, S. Levasseur, P. Carlach, M. Van Thournout, J.-M. Tarascon and C. Masquelier, *J. Mater. Chem.*, 2009, **19**, 3979–3991.
- 10 M. Cuisinier, J. F. Martin, N. Dupré, A. Yamada, R. Kanno and D. Guyomard, *Electrochem. Commun.*, 2010, **12**, 238–241.
- 11 J.-F. Martin, M. Cuisinier, N. Dupré, A. Yamada, R. Kanno and D. Guyomard, *J. Power Sources*, 2011, **196**, 2155–2163.
- 12 X. Wu, F. R. Fronczek and L. G. Butler, *Inorg. Chem.*, 1994, **33**, 1363–1365.
- 13 A. Hönnerscheid, J. Nuss, C. Mühle and M. Jansen, *Z. Anorg. Allg. Chem.*, 2003, **629**, 312–316.
- 14 G. Rousse, J. Rodriguez-Carvajal, S. Patoux and C. Masquelier, *Chem. Mater.*, 2003, **15**, 4082–4090.
- 15 *Bio-Rad/Sadtler IR Data Collection*, BR157530, Bio-Rad Laboratories, Philadelphia, PA, USA.
- 16 V. K. Kaushik, *J. Electron Spectrosc. Relat. Phenom.*, 1991, **56**, 273–277.
- 17 S. Aduru, S. Contarini and J. W. Rabalais, *J. Phys. Chem.*, 1986, **90**, 1683–1688.
- 18 P. Zhang, Y. Wu, D. Zhang, Q. Xu, J. Liu, X. Ren, Z. Luo, M. Wang and W. Hong, *J. Phys. Chem. A*, 2008, **112**, 5406–5410.
- 19 J. A. Dean, *Lange's Handbook of Chemistry*, McGraw Hill, New York, 1999.
- 20 D. Y. W. Yu, K. Donoue, T. Inoue, M. Fujimoto and S. Fujitani, *J. Electrochem. Soc.*, 2006, **153**, A835–A839.